



The following Communications have been judged by at least two referees to be “very important papers” and will be published online at www.angewandte.org soon:

T. Lewis, M. Faubel, B. Winter, J. C. Hemminger*

CO₂ Capture in an Aqueous Solution of an Amine: Role of the Solution Interface

Y. H. Kim, S. Banta*

Complete Oxidation of Methanol in an Enzymatic Biofuel Cell by a Self-Assembling Hydrogel Created from Three Modified Dehydrogenases

S. Kawamorita, H. Ohmiya, T. Iwai, M. Sawamura*

Palladium-Catalyzed Borylation of Sterically Demanding Aryl Halides with a Silica-Supported Compact Phosphane Ligand

F. Freire, A. M. Almeida, J. D. Fisk, J. D. Steinkruger, S. H. Gellman*

Impact of Strand Length on the Stability of Parallel- β -Sheet Secondary Structure

K. A. B. Austin, E. Herdtweck, T. Bach*

Intramolecular [2+2]-Photocycloaddition of Substituted Isoquinolones: Enantioselectivity and Kinetic Resolution Induced by a Chiral Template

S.-H. Kim, D. A. Weitz*

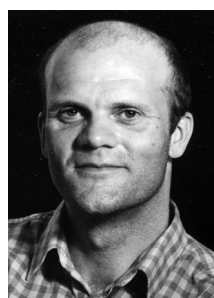
One-Step Emulsification of Multiple Concentric Shells with Capillary Microfluidic Devices

L. Furst, J. M. R. Narayanam, C. R. J. Stephenson*

Total Synthesis of (+)-Gliocladin C Enabled by Visible-Light Photoredox Catalysis

A.-L. Fameau, A. Saint-Jalmes, F. Cousin, B. H. Houssou, B. Novales, L. Navailles, F. Nallet, C. Gaillard, F. Boué, J.-P. Douliez*

Smart Foams: Reversible Switching between Ultrastable and Unstable Foams



“When I was eighteen I wanted to be an astronaut—the ultimate travel experience.

Young people should study chemistry because it is the science that strives to achieve complete understanding and control over matter, that is, the world we live in. ...”

This and more about Sjoerd Harder can be found on page 7978.

Author Profile

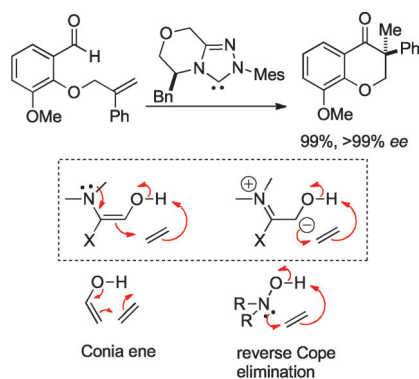
Sjoerd Harder _____ 7978

Functional Supramolecular Architectures

Paolo Samorì, Franco Cacialli

Books

reviewed by M. Mayor _____ 7979



N-Heterocyclic carbenes interact with aldehydes to generate the Breslow intermediate, a rendering of the prototypical electrophile into a nucleophile (umpolung). Recent work has indicated that these intermediates may also add to simple, unpolarized alkenes. The use of a chiral precatalyst leads to the generation of the derived adducts with high yields and very high selectivities.

Highlights

Asymmetric Organocatalysis

D. A. DiRocco, T. Rovis* — 7982–7983

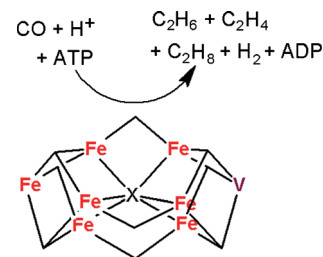
Organocatalytic Hydroacylation of Unactivated Alkenes

Vanadium Nitrogenase

D. L. Gerlach, N. Lehnert* — 7984–7986

Fischer–Tropsch Chemistry at Room Temperature?

The unique catalytic activity of vanadium nitrogenase suggests a new direction for the direct production of biofuels from CO with either synthetic catalysts or nitrogenase-containing bacteria. The reduction of CO by V nitrogenase to light hydrocarbons (see scheme) shows striking similarities to the established Fischer–Tropsch process; however, the enzyme does not use H₂ directly for this reaction. ADP = adenosine diphosphate, ATP = adenosine triphosphate.

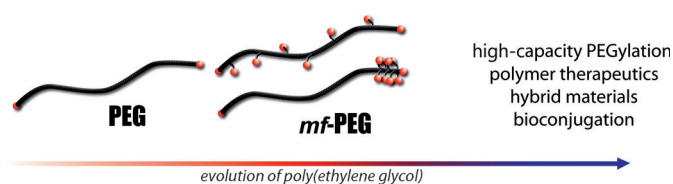


Minireviews

Functional Materials

B. Obermeier, F. Wurm, C. Mangold, H. Frey* — 7988–7997

Multifunctional Poly(ethylene glycol)s



End groups are not enough: At multi-disciplinary interfaces polymers with high loading capacity are often required, for example, for the preparation of anticancer drug conjugates. With multiple functionalities at the backbone (see picture,

red = functional group), introduced by living anionic copolymerization of ethylene oxide with an appropriate comonomer, multifunctional poly(ethylene glycol) (PEG) derivatives significantly extend the scope of the “gold standard” PEG.

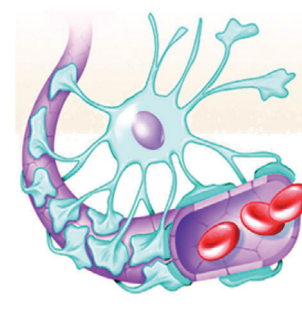
Reviews

Drug Delivery

M. Malakoutikhah, M. Teixidó*, E. Giralt* — 7998–8014

Shuttle-Mediated Drug Delivery to the Brain

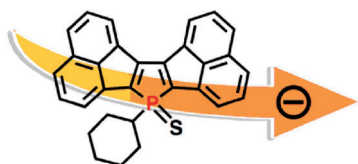
Operating a shuttle service: The use of chemical shuttles to deliver drugs to the brain is a plausible solution to overcome the obstacle posed by the blood–brain barrier. The drug is conjugated to a shuttle molecule that has the ability to permeate the blood–brain barrier (see picture).



For the USA and Canada: ANGEWANDTE CHEMIE International Edition (ISSN 1433-7851) is published weekly by Wiley-VCH, PO Box 191161, 69451 Weinheim, Germany. Air freight and mailing in the USA by Publications Expediting Inc., 200 Meacham Ave., Elmont, NY 11003. Periodicals

postage paid at Jamaica, NY 11431. US POSTMASTER: send address changes to *Angewandte Chemie*, Journal Customer Services, John Wiley & Sons Inc., 350 Main St., Malden, MA 02148-5020. Annual subscription price for institutions: US\$ 11,738/10,206 (valid for print and electronic / print or electronic delivery); for

individuals who are personal members of a national chemical society prices are available on request. Postage and handling charges included. All prices are subject to local VAT/sales tax.



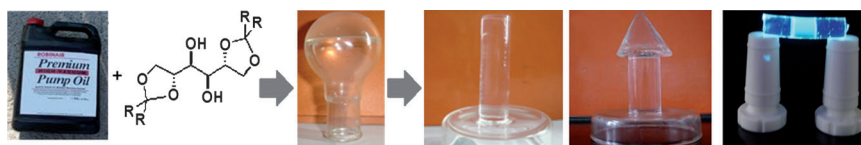
A profusion of phospholes: Diacenaphtho[1,2-*b*:1',2'-*d*]phospholes, a new class of arene-fused phosphole π -systems, were synthesized and their structural and electrochemical properties studied. The P-sulfide derivative (see picture) has a high electron-transporting ability ($\mu_E = 2.4 \times 10^{-3} \text{ cm}^2 \text{ V}^{-1} \text{ s}^{-1}$) in a vacuum-deposited film.

Communications

Extended π -Systems

Y. Matano,* A. Saito, T. Fukushima, Y. Tokudome, F. Suzuki, D. Sakamaki, H. Kaji, A. Ito, K. Tanaka, H. Imahori _____ **8016–8020**

Fusion of Phosphole and 1,1'-Biacenaphthene: Phosphorus(V)-Containing Extended π -Systems with High Electron Affinity and Electron Mobility



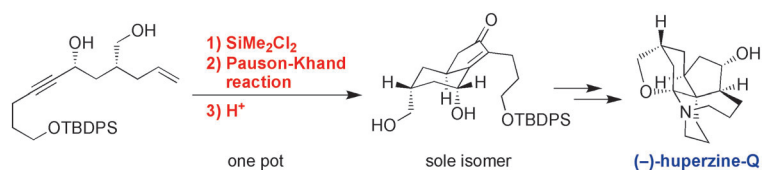
Sweet and low: Two sugar-based supergelators can congeal oils to produce highly transparent gels with glass-like refractive indices showing low UV transmittance and high visible transmittance

and remarkable self-healing properties. This unique blend of properties can be exploited to make soft optical devices from these gels.

Organogels

A. Vidyasagar, K. Handore, K. M. Sureshan* _____ **8021–8024**

Soft Optical Devices from Self-Healing Gels Formed by Oil and Sugar-Based Organogelators



Right on Q: The first asymmetric total synthesis of (–)-huperzine-Q, which possesses six stereogenic centers and a spiroaminal moiety, has been achieved in 19 steps and 16.4% overall yield. This

synthesis involved a novel stereoselective Pauson–Khand reaction, a vinyl Claisen rearrangement, and a biomimetic spiroaminal formation. TBDPS = *tert*-butyldiphenylsilyl.

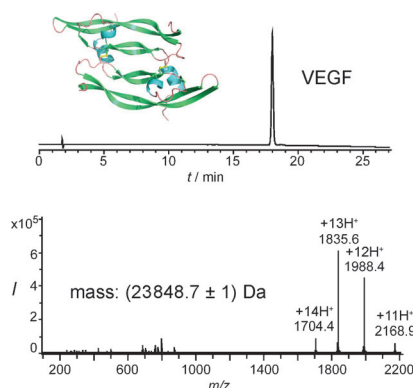
Natural Products

A. Nakayama, N. Kogure, M. Kitajima, H. Takayama* _____ **8025–8028**

Asymmetric Total Synthesis of a Pentacyclic *Lycopodium* Alkaloid: Huperzine-Q



Efficient access: The 204-residue covalent-dimer vascular endothelial growth factor (VEGF, see picture) with full mitogenic activity was prepared from three unprotected peptide segments by one-pot native chemical ligations. The covalent structure of the synthetic VEGF was confirmed by precise mass measurement, and the three-dimensional structure of the synthetic protein was determined by high-resolution X-ray crystallography.



Chemical Protein Synthesis

K. Mandal, S. B. H. Kent* _____ **8029–8033**

Total Chemical Synthesis of Biologically Active Vascular Endothelial Growth Factor

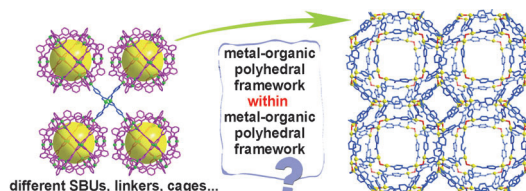


Metal–Organic Frameworks

S.-T. Zheng, T. Wu, B. Irfanoglu, F. Zuo,
P. Feng,* X. Bu* — 8034–8037



Multicomponent Self-Assembly of a
Nested $\text{Co}_{24}@\text{Co}_{48}$ Metal–Organic
Polyhedral Framework



A tale of two polyhedra: Two nested Archimedean metal–organic polyhedra, a rhombicuboctahedron (Co_{48} cage) and a cuboctahedron (Co_{24} cage), have been assembled from two types of cobalt dimers and two complementary ligands.

Within the 3D covalent cubic array of outer Co_{48} cages and framework lie encapsulated inner Co_{24} cages that are linked into a separate “hidden” 3D framework.

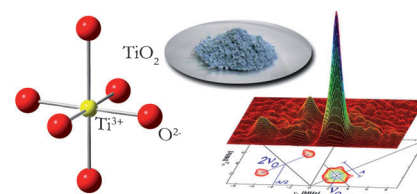
EPR Spectroscopy

S. Livraghi, S. Maurelli, M. C. Paganini,
M. Chiesa, E. Giamello* — 8038–8040



Probing the Local Environment of Ti^{3+}
Ions in TiO_2 (Rutile) by ^{17}O HSCORE

Reduced states in TiO_2 : ^{17}O hyperfine sublevel correlation spectroscopy was used to monitor the local environment of stable Ti^{3+} ions generated in a ^{17}O -enriched polycrystalline TiO_2 (rutile) sample (see picture). A hyperfine interaction of about 8 MHz is found, which is analogous to that observed for molecular Ti^{3+} aqua complex cations and suggests a localized nature of the unpaired electron wave function for these centers at 4 K.

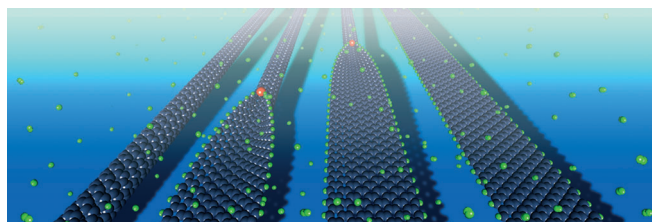


Carbon Nanotubes

J. Wang,* L. Ma, Q. Yuan, L. Zhu,
F. Ding* — 8041–8045



Transition-Metal-Catalyzed Unzipping of
Single-Walled Carbon Nanotubes into
Narrow Graphene Nanoribbons at Low
Temperature



Open, sesame! Graphene nanoribbons (GNRs) with smooth edges and controllable widths are crucial for graphene electronic and spintronic applications. High-quality narrow GNRs can be syn-

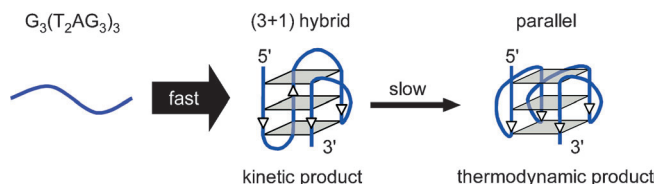
thesized from single-walled carbon nanotubes at 200–300°C using a Cu-atom catalyst, which dramatically reduces the energy barrier of unzipping from 3.11 to 1.16 eV.

DNA Structures

Y. Xue, J.-q. Liu, K.-w. Zheng, Z.-y. Kan,
Y.-h. Hao, Z. Tan* — 8046–8050



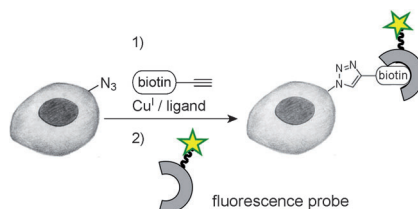
Kinetic and Thermodynamic Control of G-
Quadruplex Folding



A matter of speed: When allowed to fold in a K^+ /poly(ethylene glycol) solution, the guanine (G)-rich strand of vertebrate telomere DNA forms a parallel/antiparallel G-quadruplex, which is a (3 + 1) hybrid, within microseconds before slowly trans-

forming into the parallel one within hours (see picture). Thus, the conformation that a G-quadruplex initially adopts under physiological conditions may not be the one it adopts at the equilibrium state.

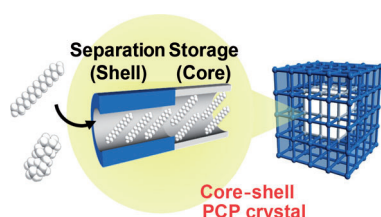
Raising the bar: The efficacy of bioorthogonal reactions for bioconjugation has been thoroughly evaluated in four different biological settings. Powered by the development of new biocompatible ligands, the copper-catalyzed azide–alkyne cycloaddition (see picture) has brought about unsurpassed bioconjugation efficiency, and thus it holds great promise as a highly potent and adaptive tool for a broader spectrum of biological applications.



Bioconjugation

C. Besanceney-Webler, H. Jiang, T. Zheng, L. Feng, D. Soriano del Amo, W. Wang, L. M. Klivansky, F. L. Marlow,* Y. Liu,* P. Wu* **8051–8056**

Increasing the Efficacy of Bioorthogonal Click Reactions for Bioconjugation: A Comparative Study

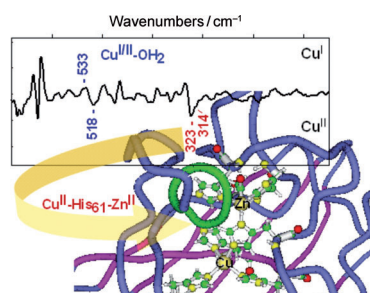


Crystal extractor: Heterostructured porous coordination polymer crystals fabricated using epitaxial growth have two contradictory porous functions, namely size selectivity and high storage. The crystals not only extract linear petroleum molecules from a mixture with its branched isomer, even at very low concentrations of linear isomer (1 wt%), but also shows improved accumulation of the molecules in its pores.

Metal–Organic Frameworks

K. Hirai, S. Furukawa,* M. Kondo, H. Uehara, O. Sakata, S. Kitagawa* **8057–8061**

Sequential Functionalization of Porous Coordination Polymer Crystals

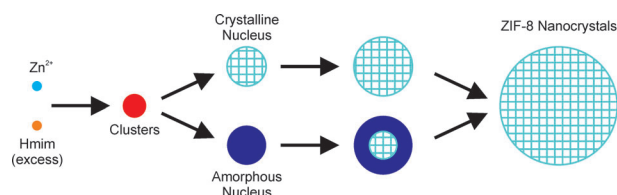


Vibrations of the metal active site of the Cu,Zn-superoxide dismutase enzyme were analyzed by far-infrared difference spectroscopy (see picture) and theoretical normal mode calculation. Both electrochemically triggered Cu^I and Cu^{II} redox states show well-defined infrared vibrational modes, notably modes of the histidine ligands, the Cu^{II}-His₆₁-Zn^{II} bridge and of the water pseudo-ligand.

Far-Infrared Spectroscopy

L. Marboutin, H. Petitjean, B. Xerri, N. Vita, F. Dupeyrat, J.-P. Flament, D. Berthomieu,* C. Berthomieu* **8062–8066**

Profiling the Active Site of a Copper Enzyme through Its Far-Infrared Fingerprint



Prenucleation clusters: In situ synchrotron X-ray scattering with a one-second time resolution revealed the occurrence of nano-sized clusters during the nucleation and early growth of nanocrystals of a

zeolitic imidazolate framework (ZIF). The complex crystallization process exhibits similarities with crystallization processes of zeolites from solution. Hmim = 2-methylimidazole.

Metal–Organic Frameworks

J. Cravillon, C. A. Schröder, R. Nayuk, J. Gummel, K. Huber,* M. Wiebcke* **8067–8071**

Fast Nucleation and Growth of ZIF-8 Nanocrystals Monitored by Time-Resolved In Situ Small-Angle and Wide-Angle X-Ray Scattering

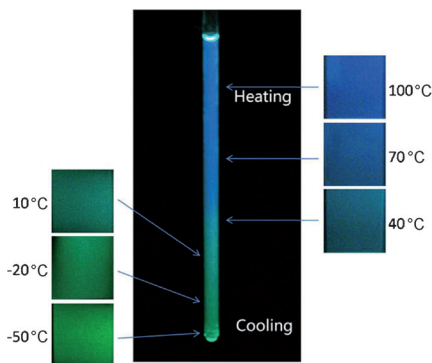


Fluorescence

J. Feng, K. J. Tian, D. H. Hu, S. Q. Wang,
S. Y. Li,* Y. Zeng, Y. Li,*
G. Q. Yang* ————— **8072–8076**



A Triarylboron-Based Fluorescent
Thermometer: Sensitive Over a Wide
Temperature Range



Feeling blue: The luminescence of a triarylboron compound has a high quantum yield (at least 0.64) over a wide temperature range (–50 to +100 °C) and changes from green to blue as the temperature is increased (see picture). The luminescence color was determined by the population of the two distinct excited-state conformations—a local excited state (high temperature) and a twisted intramolecular charge-transfer state (low temperature).

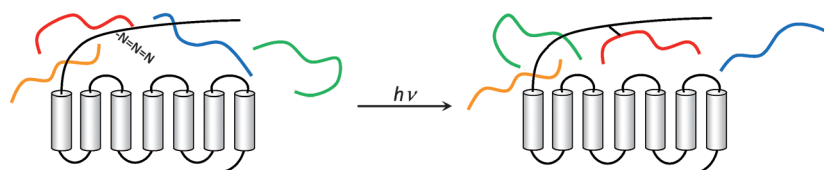


Biotransformations

I. Coin, M. H. Perrin, W. W. Vale,
L. Wang* ————— **8077–8081**



Photo-Cross-Linkers Incorporated into G-
Protein-Coupled Receptors in Mammalian
Cells: A Ligand Comparison



Capturing the right ligand at the right spot: A well-balanced system for non-natural amino acid mutagenesis allows the ligand binding sites of a class II G-

protein coupled receptor to be mapped and distinct binding domains to be identified for different ligands in the native environment of mammalian cells.

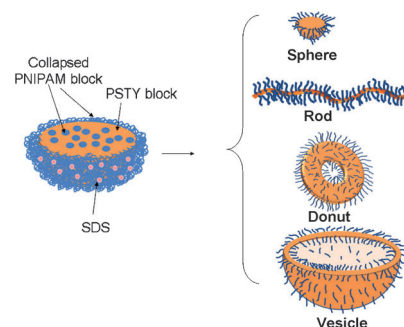
Polymer Nanostructures

S. Kessel, C. N. Urbani,
M. J. Monteiro* ————— **8082–8085**



Mechanically Driven Reorganization of
Thermoresponsive Diblock Copolymer
Assemblies in Water

Controlled formation of a variety of 3D structures was observed at high polymer weight fractions in water from a single diblock, consisting of poly(*N*-isopropylacrylamide), PNIPAM, and polystyrene, PSTY segments. The structures form through a mechanical process driven by swelling of hydrophilic polymer segments upon a change in temperature (see picture, SDS = sodium dodecylsulfate).

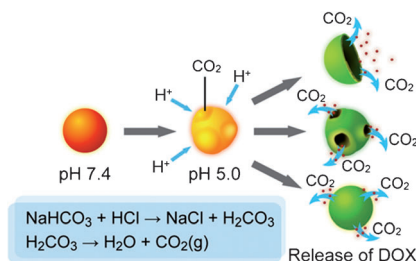


Drug Delivery

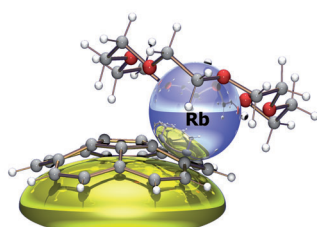
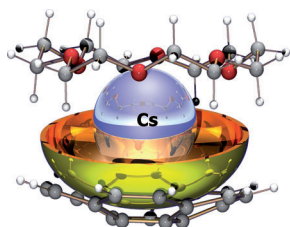
C. J. Ke, T. Y. Su, H. L. Chen, H. L. Liu,
W. L. Chiang, P. C. Chu, Y. Xia,*
H. W. Sung* ————— **8086–8089**



Smart Multifunctional Hollow
Microspheres for the Quick Release of
Drugs in Intracellular Lysosomal
Compartments



Prepared to self-destruct: When poly(*D,L*-lactic-co-glycolic acid) (PLGA) hollow microspheres containing NaHCO₃ entered the endocytic organelles of a live cell, the NaHCO₃ in the aqueous core reacted with protons that infiltrated from the compartment to generate CO₂ gas. The evolution of CO₂ bubbles led to the formation of small holes in the PLGA shell and thus rapid release of the encapsulated drug doxorubicin (DOX; see picture).



The ion size matters: The structures of corannulene monoanions crystallized with Cs⁺ and Rb⁺ ions in the presence of [18]crown-6 reveal the intrinsic binding preferences of alkali metals and allow evaluation of the bowl deformation

caused by negative charge distribution and metal binding. The large cesium cation coordinates exclusively to the concave face of C₂₀H₁₀[−], whereas the smaller rubidium cation exhibits convex binding.

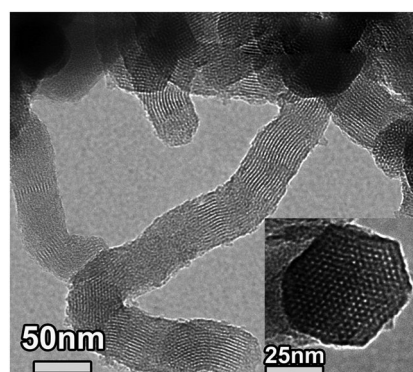
Complexation

S. N. Spisak, A. V. Zabula, A. S. Filatov,
 A. Y. Rogachev,
 M. A. Petrukhina* 8090–8094

Selective *Endo* and *Exo* Binding of Alkali Metals to Corannulene



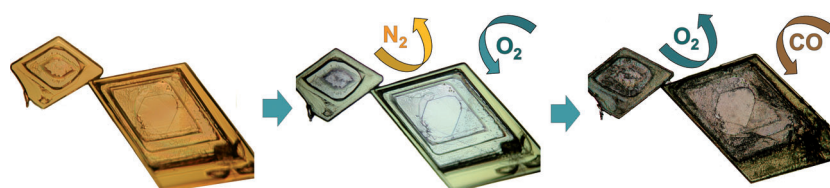
Helical organosilica materials were synthesized for the first time using a novel binaphthyl-based chiral co-monomer in less than 1 hour. The incorporation of a chiral co-monomer in the wall was shown to influence the curvature of the helical materials. As the amount of the chiral co-monomer was increased, the degree of curvature increased, illustrating the importance of this monomer to the overall morphology.



Microporous Materials

X. Wu, T. Blackburn, J. D. Webb,
 A. E. Garcia-Bennett,
 C. M. Crudden* 8095–8099

The Synthesis of Chiral Periodic Organosilica Materials with Ultrasmall Mesopores



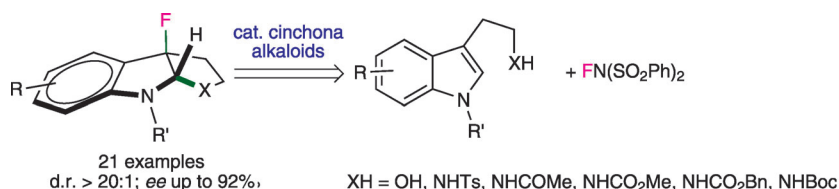
Three gases, one crystal: Rhodium NHC complexes undergo back-to-back single-crystal-to-single-crystal transformations by selective nonreversible ligand exchange

reactions (see picture). Slow diffusion of O₂ converts a dinitrogen complex into a dioxygen complex, and CO subsequently replaces O₂.

Single-Crystal Reactions

O. V. Zenkina, E. C. Keske, R. Wang,
 C. M. Crudden* 8100–8104

Double Single-Crystal-to-Single-Crystal Transformation and Small-Molecule Activation in Rhodium NHC Complexes



Enantioenriched fluorinated heterocycles can be prepared through fluorocyclizations of prochiral indoles (see scheme; Ts = tosyl, Bn = benzyl, Boc = *tert*-butoxycarbonyl). More than twenty examples for this cascade fluorination–cyclization,

which is catalyzed by cinchona alkaloids and employs *N*-fluorobenzenesulfonamide as the electrophilic fluorine source have been explored, and an unprecedented catalytic asymmetric difluorocyclization has also been identified.

Asymmetric Catalysis

O. Lozano, G. Blessley,
 T. Martinez del Campo, A. L. Thompson,
 G. T. Giuffredi, M. Bettati, M. Walker,
 R. Borman, V. Gouverneur* 8105–8109

Organocatalyzed Enantioselective Fluorocyclizations

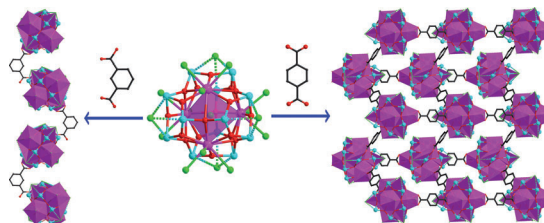


Cluster Compounds

B. Hu, M.-L. Feng, J.-R. Li, Q.-P. Lin, X.-Y. Huang* **8110–8113**



Lanthanide Antimony Oxohalides: From Discrete Nanoclusters to Inorganic–Organic Hybrid Chains and Layers



Structures à la carte: The combination of lone pairs and halide ions yields a praseodymium antimony oxohalide nanocluster $[\text{Pr}_4\text{Sb}_{12}\text{O}_{18}\text{Cl}_{17}]^{5-}$ with nearly perfect T_d symmetry. Inorganic–organic hybrid compounds with 1D chain struc-

ture and 2D wave layer structure were assembled using dicarboxylic ligands with angular or linear geometry to interconnect the nanoclusters as secondary building units (see picture; purple Pr, red O, blue Sb, green Cl).

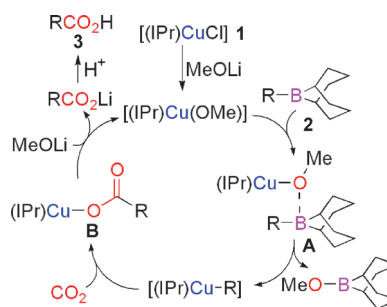
Carbon Dioxide Fixation

T. Ohishi, L. Zhang, M. Nishiura, Z. Hou* **8114–8117**



Carboxylation of Alkylboranes by N-Heterocyclic Carbene Copper Catalysts: Synthesis of Carboxylic Acids from Terminal Alkenes and Carbon Dioxide

Caught in the act: N-Heterocyclic carbene copper(II) complexes (**1**; IPr = 1,3-bis(2,6-diisopropylphenyl)imidazol-2-ylidene) serve as an excellent catalyst for the carboxylation of alkylboranes (**2**; R = alkyl) with CO_2 to afford a variety of functionalized carboxylic acids (**3**) in high yields. A novel copper methoxide/alkylborane adduct (**A**) and its subsequent CO_2 insertion product (**B**) have been isolated and shown to be true active catalyst species.

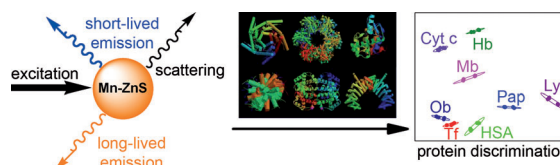


Protein Sensors

P. Wu, L.-N. Miao, H.-F. Wang, X.-G. Shao, X.-P. Yan* **8118–8121**



A Multidimensional Sensing Device for the Discrimination of Proteins Based on Manganese-Doped ZnS Quantum Dots



Lab-on-a-nanoparticle: The triple-channel optical properties of Mn-doped ZnS quantum dots (fluorescence, phosphorescence, and light scattering) are explored

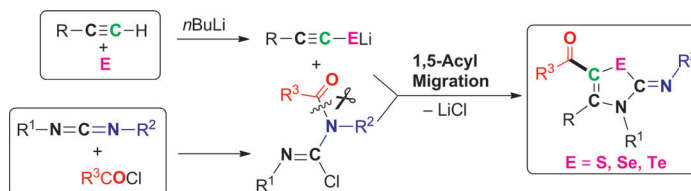
to develop a multidimensional sensing device for the discrimination of proteins in a lab-on-a-nanoparticle approach (see picture).

Synthetic Methods

Y. Wang, W.-X. Zhang,* Z. Wang, Z. Xi* **8122–8126**

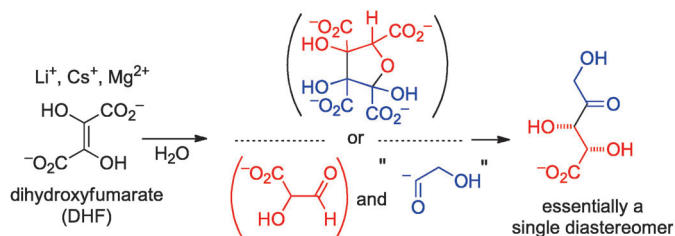


Procedure-Controlled Selective Synthesis of 5-Acyl-2-iminothiazolines and their Selenium and Tellurium Derivatives by Convergent Tandem Annulation



Concise and selective: The procedure-controlled synthesis of the title compounds has been achieved for the first time by an organolithium-promoted convergent tandem annulation involving

readily available terminal alkynes, chalcogen elements (S, Se, and Te), carbodiimides, and acid chlorides. A novel 1,5-acyl migration is considered to be essential for this useful transformation.



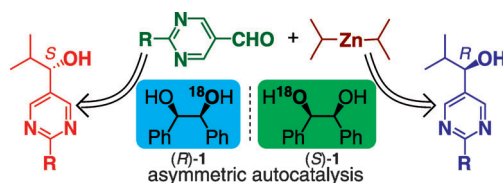
Jack of all trades: Water-soluble salts of DHF underwent self-condensation to afford the *threo* diastereomer of pentulosonic acid, through differing reaction pathways contingent on the metal salt

used (see scheme). This transformation exemplifies the diverging roles of DHF as a nucleophile (a synthon for α -hydroxyacetyl anion) and an electrophile (an α -carboxyglycolaldehyde equivalent).

Prebiotic Chemistry

V. Naidu Sagi, P. Karri, F. Hu,
 R. Krishnamurthy* — 8127–8130

Diastereoselective Self-Condensation of Dihydroxyfumaric Acid in Water: Potential Route to Sugars



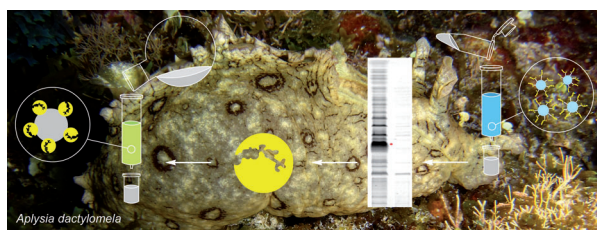
Trigger happy: Chiral oxygen isotopomers of hydrobenzoin ($[^{18}\text{O}](R)$ -1 and $[^{18}\text{O}](S)$ -1) acted as chiral triggers to induce the enantioselective addition of $i\text{Pr}_2\text{Zn}$ to pyrimidine-5-carbaldehyde. An extremely

small chiral influence arising from the presence of the oxygen isotope (^{18}O) is amplified through asymmetric autocatalysis to enantioenrich the 5-pyrimidyl alkanol product.

Asymmetric Induction

T. Kawasaki,* Y. Okano, E. Suzuki,
 S. Takano, S. Oji, K. Soai* — 8131–8133

Asymmetric Autocatalysis: Triggered by Chiral Isotopomer Arising from Oxygen Isotope Substitution



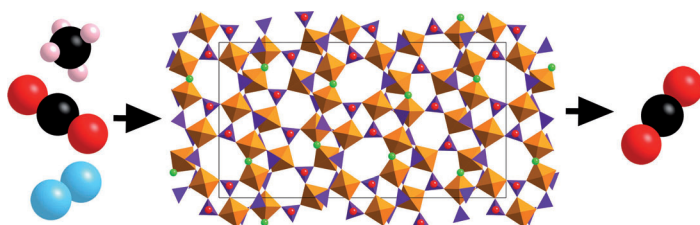
A bidirectional affinity system has been developed for the identification of cancer-related natural products and their biological targets. Aplysqualenol A is thus selectively identified as a ligand of the dynein light chain. The use of forward and

reverse affinity methods suggests that both small-molecule isolation and target identification can be conducted using conventional molecular biological methods.

Natural Product Binding

B. Vera, A. D. Rodríguez,*
 J. J. La Clair* — 8134–8138

Aplysqualenol A Binds to the Light Chain of Dynein Type 1 (DYNLL1)



Less is more: An open-framework zirconium phosphate with unusual 7-ring channels was synthesized ionothermally from a deep-eutectic solvent. This small-pore material displays a CO_2/CH_4

adsorption ratio (17.3 at 1 bar) that is significantly higher than that of typical 8-ring materials, making it highly attractive for CO_2/CH_4 separations.

Ionothermal Synthesis

L. Liu, J. F. Yang, J. P. Li, J. X. Dong,*
 D. Šišak, M. Luzzatto,
 L. B. McCusker* — 8139–8142

Ionothermal Synthesis and Structure Analysis of an Open-Framework Zirconium Phosphate with a High CO_2/CH_4 Adsorption Ratio



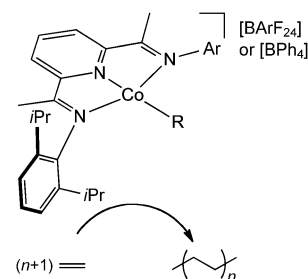
Polymerization Catalysts

C. C. Hojilla Atienza, C. Milschmann,
E. Lobkovsky, P. J. Chirik* — 8143–8147



Synthesis, Electronic Structure, and
Ethylene Polymerization Activity of
Bis(imino)pyridine Cobalt Alkyl Cations

A new spin on polymers: The title cations comprise low-spin Co^{II} centers with neutral bis(imino)pyridine chelating ligands. These complexes serve as single-component ethylene polymerization catalysts (see scheme) and offer insight into the mechanism of chain growth and catalyst deactivation, which occurs by forming inactive cationic bis(imino)pyridine cobalt complexes with a diethyl ether ligand.

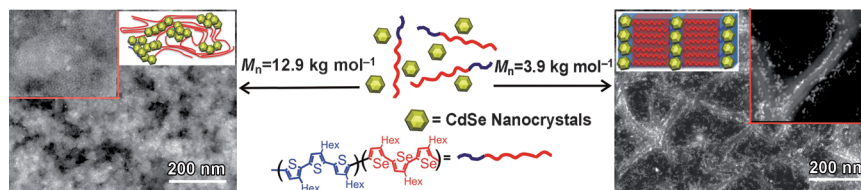


Semiconducting Nanocomposites

L. Li, J. Hollinger, N. Coombs, S. Petrov,
D. S. Seferos* — 8148–8152



Nanocrystal Self-Assembly with Rod–Rod
Block Copolymers



Two distinct morphologies of hexylsele-nophene–hexylthiophene rod–rod block copolymer films can be prepared depending on the molecular weight of the sample (see picture: left $M_n = 12.9$, right

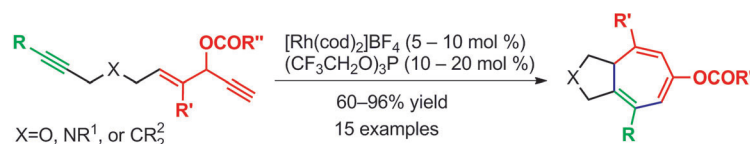
$M_n = 3.9 \text{ kg mol}^{-1}$). These polymers can be used to organize spherical CdSe nanocrystals (yellow) into either dispersed or aligned hierarchical structures. Scale bars: 200 nm.

Cycloisomerization

X.-z. Shu, S. Huang, D. Shu, I. A. Guzei,
W. Tang* — 8153–8156



Interception of a Rautenstrauch
Intermediate by Alkynes for [5+2]
Cycloaddition: Rhodium-Catalyzed
Cycloisomerization of 3-Acyloxy-4-ene-1,9-
diynes to Bicyclo[5.3.0]decatrienes



Rholling in the bicycles: A rhodium(I)-catalyzed cycloisomerization for the synthesis of bicyclic compounds containing a cycloheptatriene ring from linear alkenynes (see scheme; cod = 1,5-cyclo-octadiene) is proposed to proceed

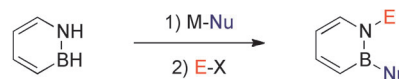
through 1,2-acyloxy migration, 6 π electrocyclicization, migratory insertion, and reductive elimination. The overall process can be viewed as a novel intramolecular [5+2] cycloaddition with concomitant 1,2-acyloxy migration.

Heterocycles

A. N. Lamm, E. B. Garner, III, D. A. Dixon,
S.-Y. Liu* — 8157–8160

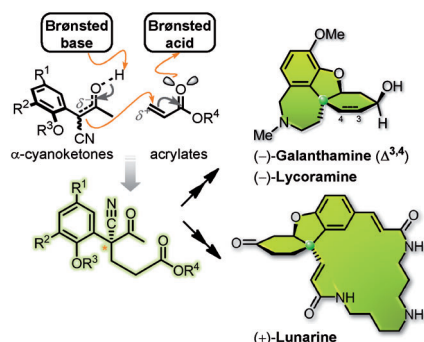


Nucleophilic Aromatic Substitution
Reactions of 1,2-Dihydro-1,2-Azaborine



Could go either way: The addition of nucleophiles to the parent 1,2-dihydro-1,2-azaborine and subsequent quenching with an electrophile generates novel substituted 1,2-azaborine derivatives (see

scheme). Mechanistic studies are consistent with two distinct nucleophilic aromatic substitution pathways depending on the nature of the nucleophile.

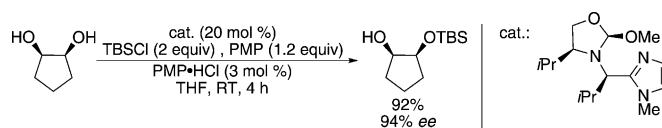


Divergent route: A direct C–C bond-forming approach to the key aryl-substituted all-carbon quaternary stereogenic center present in bioactive hydrodibenzofuran alkaloids has been discovered. This approach involves an unprecedented organocatalytic enantioselective Michael addition of α -cyanoketones with acrylates (see scheme) and was used in a novel and divergent synthetic strategy for the title compounds in asymmetric fashion.

Organocatalysis

P. Chen, X. Bao, L.-F. Zhang, M. Ding, X.-J. Han, J. Li, G.-B. Zhang, Y.-Q. Tu, C.-A. Fan* **8161–8166**

Asymmetric Synthesis of Bioactive Hydrodibenzofuran Alkaloids: (–)-Lycoramine, (–)-Galanthamine, and (+)-Lunarine



Ex-changing places: A highly enantioselective desymmetrization of 1,2-diols has been developed in which the catalyst utilizes reversible covalent bonding to the substrate to achieve both high selectivity and rate acceleration (see scheme,

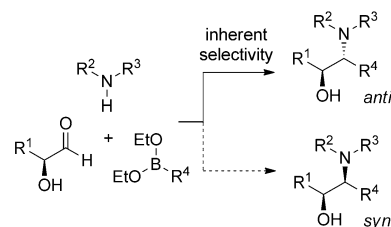
PMP = pentalmethylpiperidine, TBS = *tert*-butyldimethylsilyl). Induced intramolecularity is responsible for the enhanced rate, thus allowing the reaction to be performed at room temperature.

Organocatalysis

X. Sun, A. D. Worthy, K. L. Tan* **8167–8171**

Scaffolding Catalysts: Highly Enantioselective Desymmetrization Reactions

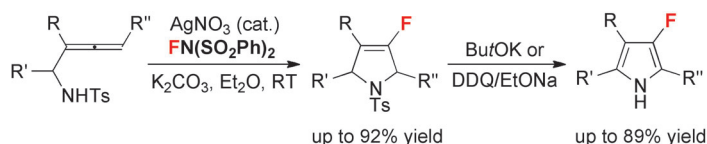
Multicomponent Petasis reactions: The first diastereoselective Petasis reaction catalyzed by chiral biphenols that enables the synthesis of *syn* and *anti* β -amino alcohols in pure form has been developed. The reaction exploits a multicomponent approach that involves boronates, α -hydroxy aldehydes, and amines (see scheme).



Multicomponent Reactions

G. Muncipinto, P. N. Moquist, S. L. Schreiber, S. E. Schaus* **8172–8175**

Catalytic Diastereoselective Petasis Reactions



A nice combination: The intramolecular oxidative amino-fluorination of allenes using silver catalysis and $\text{FN}(\text{SO}_2\text{Ph})_2$ as the fluorinating reagent has been developed. This reaction represents an efficient

method for the synthesis of various 4-fluoro-2,5-dihydropyrrole compounds. Further transformation provided the corresponding fluorinated pyrrole derivatives in good yields (see scheme).

Organofluorine Chemistry

T. Xu, X. Mu, H. Peng, G. Liu* **8176–8179**

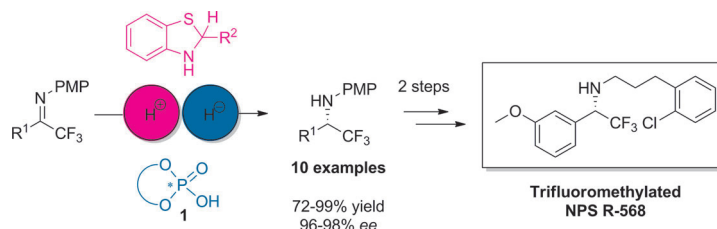
Silver-Catalyzed Intramolecular Amino-fluorination of Activated Allenes

Synthetic Methods

A. Henseler, M. Kato, K. Mori,
T. Akiyama* — 8180–8183



Chiral Phosphoric Acid Catalyzed Transfer Hydrogenation: Facile Synthetic Access to Highly Optically Active Trifluoromethylated Amines



Amines to an end: Highly optically active α -CF₃-functionalized amines can be obtained using metal-free reaction conditions. The method involves the transfer hydrogenation of CF₃-substituted ketones catalyzed by **1** and reductive ami-

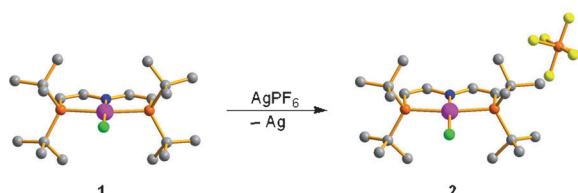
nation of CF₃-substituted ketones. The synthetic utility of this method was demonstrated by the synthesis of a CF₃ analogue of NPS R-568. PMP = *para*-methoxyphenyl.

Square-Planar Iridium(III)

J. Meiners, M. G. Scheibel,
M.-H. Lemée-Cailleau, S. A. Mason,
M. B. Boeddinghaus, T. F. Fässler,
E. Herdtweck, M. M. Khusniyarov,*
S. Schneider* — 8184–8187



Square-Planar Iridium(II) and Iridium(III) Amido Complexes Stabilized by a PNP Pincer Ligand



Squaring the circle: The novel dienamido pincer ligand N(CHCHP*t*Bu₂)₂[−] affords the isolation of the unusual square-planar iridium(II) and iridium(III) amido complexes [IrCl{N(CHCHP*t*Bu₂)₂}]^{*n*} (*n* = 0 (**1**),

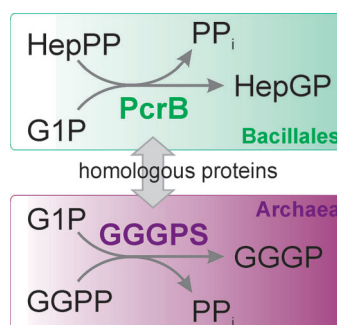
+1 (**2**)). In contrast, the corresponding iridium(I) complex of the redox series (*n* = −1) is surprisingly unstable. The diamagnetism of **2** is attributed to strong N → Ir π donation.

Enzyme Discovery

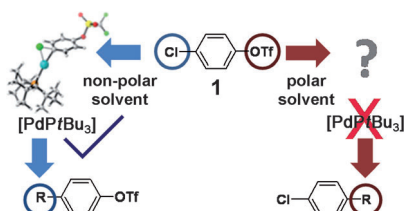
H. Guldán, F.-M. Matysik, M. Bocola,
R. Sterner, P. Babinger* — 8188–8191



Functional Assignment of an Enzyme that Catalyzes the Synthesis of an Archaea-Type Ether Lipid in Bacteria



An archaea-type ether lipid in bacteria: PcrB, the bacterial homologue of the archaea-specific geranylgeranylglycerol phosphate synthase, produces heptaprenyglyceryl phosphate in bacillales. The product becomes dephosphorylated and acetylated in vivo.



Suzuki coupling of the bifunctional substrate **1** using $[\text{Pd}_2(\text{dba})_3]/\text{PtBu}_3$ gives selectivity for C–Cl in nonpolar solvents but for C–OTf in polar solvents. The results of computational and experimental studies suggest that the catalytically active species in polar solvents under conditions employing coordinating additives is inconsistent with monoligated $[\text{Pd}(\text{PtBu}_3)]$. Instead, the data are consistent with an anionic palladium complex as the active species.

Cross-Coupling

F. Proutiere,
F. Schoenebeck* _____ 8192–8195

Solvent Effect on Palladium-Catalyzed Cross-Coupling Reactions and Implications on the Active Catalytic Species



Supporting information is available on www.angewandte.org (see article for access details).



A video clip is available as Supporting Information on www.angewandte.org (see article for access details).



This article is available online free of charge (Open Access)

Looking for outstanding employees?

Do you need another expert for your excellent team?
... Chemists, PhD Students, Managers, Professors, Sales Representatives...
Place an advert in the printed version and have it made available online for 1 month, free of charge!

Angewandte Chemie International Edition

Advertising Sales Department: Marion Schulz

Phone: 0 62 01 - 60 65 65

Fax: 0 62 01 - 60 65 50

E-Mail: MSchulz@wiley-vch.de

Service

Spotlight on Angewandte's
Sister Journals _____ 7974–7976

Preview _____ 8197

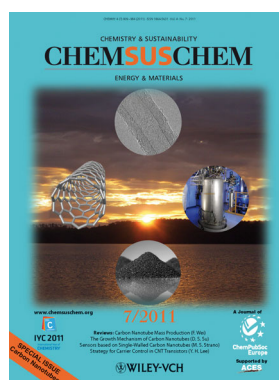
Check out these journals:



www.chemasianj.org



www.chemmedchem.org



www.chemsuschem.org



www.chemcatchem.org

Corrigenda

Synthesis of Gold Nano-hexapods with Controllable Arm Lengths and Their Tunable Optical Properties

D. Y. Kim, T. Yu, E. C. Cho, Y. Ma,
O O. Park, Y. Xia* — 6328–6331

Angew. Chem. Int. Ed. **2011**, 50

DOI 10.1002/anie.201100983

The authors of this Communication have noticed a typographical error in the experimental section of the Supporting Information. The volume of aqueous NaBH₄ solution, which was used for preparing spherical Au seeds, should be 0.6 ml rather than 6 ml. This error does not influence any other parts of the paper. The authors sincerely apologize for this mistake and any inconvenience it may have caused.

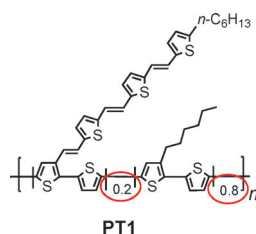
All-Polymer Solar Cells from Perylene Diimide Based Copolymers: Material Design and Phase Separation Control

E. J. Zhou, J. Z. Cong, Q. S. Wei,
K. Tajima,* C. H. Yang,
Prof.K. Hashimoto* — 2799–2803

Angew. Chem. Int. Ed. **2011**, 50

DOI 10.1002/anie.201005408

In this Communication, the structure of **PT1** is not correct in Scheme 1 on page 2799. The correct structure is shown below. Also, the ratio between the units with and without the conjugated side chain should be 0.2:0.8, not 0.8:0.2.



In the Supporting Information, the structure of **PT1** in Figure S2 on page S4 is also incorrect. The correct structure is shown above. Also, on page S14 “Monomer 4 (130 mg, 0.8 mmol)” should be corrected to “Monomer 4 (130 mg, 0.2 mmol)”.